Insights into Templated Supramolecular Polymerization: Binding of Naphthalene Derivatives to ssDNA Templates of Different Lengths

Pim G. A. Janssen,[†,§] Sara Jabbari-Farouji,[‡,§,||] Mathieu Surin,[⊥] Xavier Vila,[†]
Jeroen C. Gielen,[#] Tom F. A. de Greef,[†,§] Matthijn R. J. Vos,[†] Paul H. H. Bomans,[†]
Nico A. J. M. Sommerdijk,[†] Peter C. M. Christianen,[#] Philippe Leclère,[†,⊥]
Roberto Lazzaroni,[⊥] Paul van der Schoot,[‡] E. W. Meijer,*,[†,§] and
Albertus P. H. J. Schenning*,[†,§]

*Laboratory for Macromolecular and Organic Chemistry, Group Theoretical and Polymer
Physics, and Institute for Complex Molecular Systems, Eindhoven University of Technology,
P.O. Box 513, 5600 MB Eindhoven, The Netherlands, Dutch Polymer Institute,
P.O. Box 902, 5600 AX Eindhoven, The Netherlands, Laboratory for Chemistry of Novel
Materials, University of Mons-Hainaut, B-7000 Mons, Belgium, and High Field Magnet
Laboratory, Institute of Molecules and Materials, Radboud University Nijmegen,
Toernooiveld 7, 6525 ED Nijmegen, The Netherlands*

Received October 14, 2008; E-mail: e.w.meijer@tue.nl; a.p.h.j.schenning@tue.nl

Abstract: We report on two diaminotriazine-equipped naphthalene derivatives that bind reversibly to a single-stranded DNA template or "tape-measure molecule" via hydrogen bonding, yielding monodisperse double-stranded DNA hybrids with one strand consisting of a supramolecular naphthalene backbone. These assemblies have been investigated extensively, both experimentally and theoretically. The structure and the templated self-assembly process of the complex have been characterized with UV−vis spectroscopy, circular dichroism spectroscopy, molecular dynamics simulations, cryo-transmission electron microscopy, liquid atomic force microscopy, electrospray ionization mass spectrometry, light scattering, and ^1H NMR and infrared spectroscopy. We have found that the DNA hybrid complexes have a right-handed helical arrangement stabilized by $\pi-\pi$ interactions and hydrogen bonds. The hydrophilic hydroxyl group at the end of the ethylene glycol of the guest molecule suppressed both the nontemplated self-assembly of the naphthalene guest molecules and the further aggregation of the entire DNA hybrid complex. Through the use of a theoretical mass-action model for the templated self-assembly, the host−guest and guest−guest interaction energies were estimated by fitting to the spectroscopic data. The differently estimated values of the interaction energies and thermodynamic parameters vary within experimental error, showing the self-consistency of the model. From the obtained correlation between the positions of the guest molecules bound on the template, we have obtained a qualitative theoretical picture of the way in which the guests are physically distributed on the templates. For short templates, the templates are filled one-by-one, even at moderate fractions of bound sites. For larger templates, the templates first have alternating sequences of filled and empty sections, after which, at large fractions of bound sites, virtually all of the binding sites for all template lengths are filled.

Introduction

In nature, templates with specific binding sites are used to efficiently form assemblies and polymers with defined sizes or sequence. For instance, RNA acts as a "tape-measure" template for the assembly of coat proteins of the tobacco mosaic virus,[1] while its sequence can also be transcribed into proteins via the specific recognition of codons.[2] Nature's concept has inspired many researchers to exploit templated polymerization[3,4] as a tool for controlling the size and sequence of synthetic polymers via a "bottom-up" approach.[5] As a result, viruses,[6] biopolymers,[3,4f,g] and synthetic polymers[4b,c] have been used as templates for the self-assembly of a variety of biological, organic, and inorganic building blocks. For example, synthetic poly(trimethylene iminium)[4b] and oligo(phenylene ethynylene)[4c] templates have

[†] Laboratory for Macromolecular and Organic Chemistry, Eindhoven University of Technology.
[‡] Group Theoretical and Polymer Physics, Eindhoven University of Technology.
[§] Institute for Complex Molecular Systems, Eindhoven University of Technology.
[||] Dutch Polymer Institute.
[⊥] Laboratory for Chemistry of Novel Materials, University of Mons-Hainaut.
[#] Institute of Molecules and Materials, Radboud University Nijmegen.

(1) (a) Special Issue: Tobacco Mosaic Virus: Pioneering Research for a Century. *Philos. Trans. R. Soc London, Ser. B* **1999**, *354*, 517−685. (b) Kittel, C. *Am. J. Phys.* **1969**, *37*, 917−920.
(2) Stryer, L. *Biochemistry*, 4th revised ed.; Freeman: New York, 1996; p 1100.

been used to organize porphyrins between two strands and to bind amphiphilic peptides, respectively. Biopolymers, such as RNA and DNA, have also been used as templates to mimic their replication nonenzymatically[3b] and to create non-natural polymers with a predefined sequence.[3c] Similarly, the DNA-templated self-assembly of nanoparticles,[7] chromophores,[8] and lipids[8] has been reported. Apart from being templates, DNA and functionalized nucleotides[9] can be used as building blocks to create predefined complex nanosized structures via sticky-end cohesion.[10]

For the exploitation of templated polymerizations, it is essential to develop a deeper understanding of the binding interaction between the host template and the guest molecules and that between the guest molecules.[3,4,11] For example, to obtain a so-called all-or-nothing process in which complete templates are filled one by one, the guest−guest and host−guest interactions cannot be arbitrary. When the host−guest interaction is strong and the guest−guest interaction weak, the guest molecules are uniformly dispersed over all of the available template binding sites and therefore do not entirely fill any of the templates, except of course when the overall template coverage is very high. In the other extreme, a strong guest−guest interaction could lead to a competition between templated and nontemplated self-assembly and to very polydisperse aggregates that are potentially larger on average than the template size.

We have previously shown that two water-soluble guest molecules, a naphthalene derivative **G1** and an oligo (*p*-phenylene)vinylene diaminotriazine derivative, under appropriate conditions bind to a complementary oligothymine strand (**dT40** having 40 thymines), as evidenced by optical and electrospray ionization (ESI) studies (Scheme 1).[12] We observed that at high concentrations of the guests, nontemplated self-assembly interferes with the templated self-assembly. We here

report on the templated self-assembly of a newly designed naphthalene guest molecule **G2** on oligothymine templates of various lengths (denoted as **dT*q***, where *q* is the number of thymines), yielding objects whose size is controlled by the length of the template (Scheme 1). We have redesigned the naphthalene guest molecule **G1** to suppress the nontemplated self-assembly by replacing the methyl-terminated ethylene oxide with a hydroxyl-terminated ethylene oxide, yielding guest molecule **G2**.[13] The self-assembled structures are characterized in detail with molecular dynamics (MD) simulations, dynamic light scattering (DLS), and microscopy. Furthermore, we have developed a theoretical model for guests adsorbing to a linear template with a finite size in order to gain insight into the templated supramolecular polymerization process. With this model, we were able to analyze our experimental findings and obtain binding energies for both the host−guest and guest−guest interactions. With the obtained guest−guest interaction energy, we can determine the correlation length, i.e., the length of correlated template binding sites, which predicts the way that the guests are distributed on the template as a function of the template length.[14]

Results and Discussion

Nontemplated Self-Assembly. We first compare the nontemplated self-assembly of **G2** with the earlier reported data for

(3) Examples and reviews of templated polymerizations: (a) Gons, J.; Vorenkamp, E. J.; Challa, G. *J. Polym. Sci., Part A: Polym. Chem.* **1975**, *13*, 1699–1709. (b) Inoue, T.; Orgel, L. E. *Science* **1983**, *219*, 859–862. (c) Inoue, T.; Joyce, G. F.; Grzeskowiak, K.; Orgel, L. E.; Brown, J. M.; Reese, C. B. *J. Mol. Biol.* **1984**, *178*, 669–676. (d) Kleiner, R. E.; Brudno, Y.; Birnbaum, M. E.; Liu, D. R. *J. Am. Chem. Soc.* **2008**, *130*, 4646–4659. (e) Saito, R. *Polymer* **2008**, *49*, 2625–2631. (f) van Hest, J. C. M. *Nat. Chem. Biol.* **2008**, *4*, 272–273. (g) Clapper, J. D.; Sievens-Figueroa, L.; Guymon, C. A. *Chem. Mater.* **2008**, *20*, 768–781.

(4) Examples of templated supramolecular polymerizations: (a) Lindsey, J. S. *New J. Chem.* **1991**, *15*, 153–180. (b) Sugimoto, T.; Suzuki, T.; Shinkai, S.; Sada, K. *J. Am. Chem. Soc.* **2007**, *129*, 270–271. (c) Bull, S. R.; Palmer, L. C.; Fry, N. J.; Greenfield, M. A.; Messmore, B. W.; Meade, T. J.; Stupp, S. I. *J. Am. Chem. Soc.* **2008**, *130*, 2742–2743. (d) Ohkawa, H.; Ligthart, G. B. W. L.; Sijbesma, R. P.; Meijer, E. W. *Macromolecules* **2007**, *40*, 1453–1459. (e) Hoogenboom, R.; Fournier, D.; Schubert, U. S. *Chem. Commun.* **2008**, 155–162. (f) de la Escosura, A.; Verwegen, M.; Sikkema, F. D.; Comellas-Aragones, M.; Kirilyuk, A.; Rasing, T.; Nolte, R. J. M.; Cornelissen, J. J. L. M. *Chem. Commun.* **2008**, 1542–1544. (g) Xu, Y.; Ye, J.; Liu, H.; Cheng, E.; Yang, Y.; Wang, W.; Zhao, M.; Zhou, D.; Liu, D.; Fang, R. *Chem. Commun.* **2008**, 49–51. (h) Benvin, A. L.; Creeger, Y.; Fisher, G. W.; Ballou, B.; Waggoner, A. S.; Armitage, B. A. *J. Am. Chem. Soc.* **2007**, *129*, 2025–2034. (i) Hunter, C. A.; Tomas, S. *J. Am. Chem. Soc.* **2006**, *128*, 8975–8979.

(5) Recent examples and reviews of bottom-up approaches: (a) Service, R. F. *Science* **2005**, *309*, 95. (b) Schenning, A. P. H. J. *Synth. Met.* **2004**, *147*, 43–48. (c) Hoeben, F. J. M.; Jonkheijm, P.; Meijer, E. W.; Schenning, A. P. H. J. *Chem. Rev.* **2005**, *105*, 1491–1546. (d) Ikkala, O.; ten Brinke, G. *Chem. Commun.* **2004**, 2131–2137. (e) Ajayaghosh, A.; Praveen, V. K. *Acc. Chem. Res.* **2007**, *40*, 644–656. (f) Ligthart, G. B. W. L.; Ohkawa, H.; Sijbesma, R. P.; Meijer, E. W. *J. Am. Chem. Soc.* **2005**, *127*, 810–811. (g) Knoben, W.; Besseling, N. A. M.; Stuart, M. A. C. *Macromolecules* **2006**, *39*, 2643–2653. (h) Jonkheijm, P.; van der Schoot, P.; Schenning, A. P. H. J.; Meijer, E. W. *Science* **2006**, *313*, 80–83. (i) Smulders, M. M. J.; Schenning, A. P. H. J.; Meijer, E. W. *J. Am. Chem. Soc.* **2008**, *130*, 606–611.

(6) Examples where viruses act as templates: (a) Huang, Y.; Chiang, C.-Y.; Lee, S. K.; Gao, Y.; Hu, E. L.; De Yoreo, J.; Belcher, A. M. *Nano Lett.* **2005**, *5*, 1429–1434. (b) Mao, C.; Solis, D. J.; Reiss, B. D.; Kottmann, S. T.; Sweeney, R. Y.; Hayhurst, A.; Georgiou, G.; Iverson, B.; Belcher, A. M. *Science* **2004**, *303*, 213–217. (c) Sotiropoulou, S.; Sierra-Sastre, Y.; Mark, S. S.; Batt, C. A. *Chem. Mater.* **2008**, *20*, 821–834.

(7) Examples of DNA as a structural scaffold to organize particles: (a) Pinto, Y. Y.; Le, J. D.; Seeman, N. C.; Musier-Forsyth, K.; Taton, T. A.; Kiehl, R. A. *Nano Lett.* **2005**, *5*, 2399–2402. (b) Tang, Z.; Kotov, N. A. *Adv. Mater.* **2005**, *17*, 951–962. (c) Nykypanchuk, D.; Maye, M. M.; van der Lelie, D.; Gang, O. *Nature* **2008**, *451*, 549–552. (d) Zhang, J.; Liu, Y.; Ke, Y.; Yan, H. *Nano Lett.* **2006**, *6*, 248–251. (e) Gothelf, K. V.; LaBean, T. H. *Org. Biomol. Chem.* **2005**, *3*, 4023–4037. (f) Park, S. H.; Yin, P.; Liu, Y.; Reif, J. H.; LaBean, T. H.; Yan, H. *Nano Lett.* **2005**, *5*, 729–733.

(8) (a) Iwaura, R.; Hoeben, F. J. M.; Masuda, M.; Schenning, A. P. H. J.; Meijer, E. W.; Shimizu, T. *J. Am. Chem. Soc.* **2006**, *128*, 13298–13304. (b) Iwaura, R.; Yoshida, K.; Masuda, M.; Ohnishi-Kameyama, M.; Yoshida, M.; Shimizu, T. *Angew. Chem., Int. Ed.* **2003**, *42*, 1009–1012. (c) Iwaura, R.; Kikkawa, Y.; Ohnishi-Kameyama, M.; Shimizu, T. *Org. Biomol. Chem.* **2007**, *5*, 3450–3455.

(9) Examples of chromophores covalently linked to DNA: (a) Krueger, A. T.; Lu, H.; Lee, A. H. F.; Kool, E. T. *Acc. Chem. Res.* **2007**, *40*, 141–150. (b) Kool, E. T. *Acc. Chem. Res.* **2002**, *35*, 936–943. (c) Lewis, F. D.; Zhang, L.; Zuo, X. *J. Am. Chem. Soc.* **2005**, *127*, 10002–10003. (d) Balaz, M.; Holmes, A. E.; Benedetti, M.; Rodriguez, P. C.; Berova, N.; Nakanishi, K.; Proni, G. *J. Am. Chem. Soc.* **2005**, *127*, 4172–4173. (e) Kashida, H.; Asanuma, H.; Komiyama, M. *Angew. Chem., Int. Ed.* **2004**, *43*, 6522–6525.

(10) Examples of 2D and 3D DNA structures: (a) Seeman, N. C. *Methods Mol. Biol.* **2005**, *303*, 143–166. (b) Chen, J.; Seeman, N. C. *Nature* **1991**, *350*, 631–633. (c) Rothemund, P. W. K. *Nature* **2006**, *440*, 297–302. (d) He, Y.; Ye, T.; Su, M.; Zhang, C.; Ribbe, A. E.; Jiang, W.; Mao, C. *Nature* **2008**, *452*, 198–201.

(11) Recent reviews of template-directed reactions: (a) Pianowski, Z. L.; Winssinger, N. *Chem. Soc. Rev.* **2008**, *37*, 1330–1336. (b) MacGillivray, L. R. *J. Org. Chem.* **2008**, *73*, 3311–3317. (c) Meyer, C. D.; Joiner, C. S.; Stoddart, J. F. *Chem. Soc. Rev.* **2007**, *36*, 1705–1723. (d) Silverman, A. P.; Kool, E. T. *Chem. Rev.* **2006**, *106*, 3775–3789.

(12) (a) Janssen, P. G. A.; Vandenbergh, J.; van Dongen, J. L. J.; Meijer, E. W.; Schenning, A. P. H. J. *J. Am. Chem. Soc.* **2007**, *129*, 6078–6079. (b) Janssen, P. G. A.; van Dongen, J. L. J.; Meijer, E. W.; Schenning, A. P. H. J. *Chem.—Eur. J.* [Online early access]. DOI: 10.1002/chem.200801506. Published Online: Nov 28, 2008.

(13) Kuehne, R.; Ebert, R. U.; Kleint, F.; Schmidt, G.; Schueuermann, G. *Chemosphere* **1995**, *30*, 2061–2077.

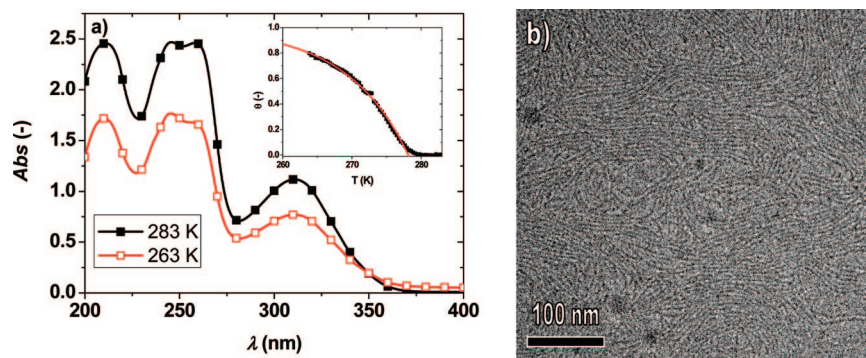(14) Zimm, B. H.; Bragg, J. K. *J. Chem. Phys.* **1959**, *31*, 526–535.

Figure 1. (a) UV spectra of a 1 mM **G2** solution at 263 and 283 K in water. The inset shows the fraction of aggregated **G2** measured at 269 nm and the fit based on the previously developed model for cooperative self-assembly.[5h] (b) Cryo-TEM image of a 1 mM **G1** solution in water vitrified at 283 K.
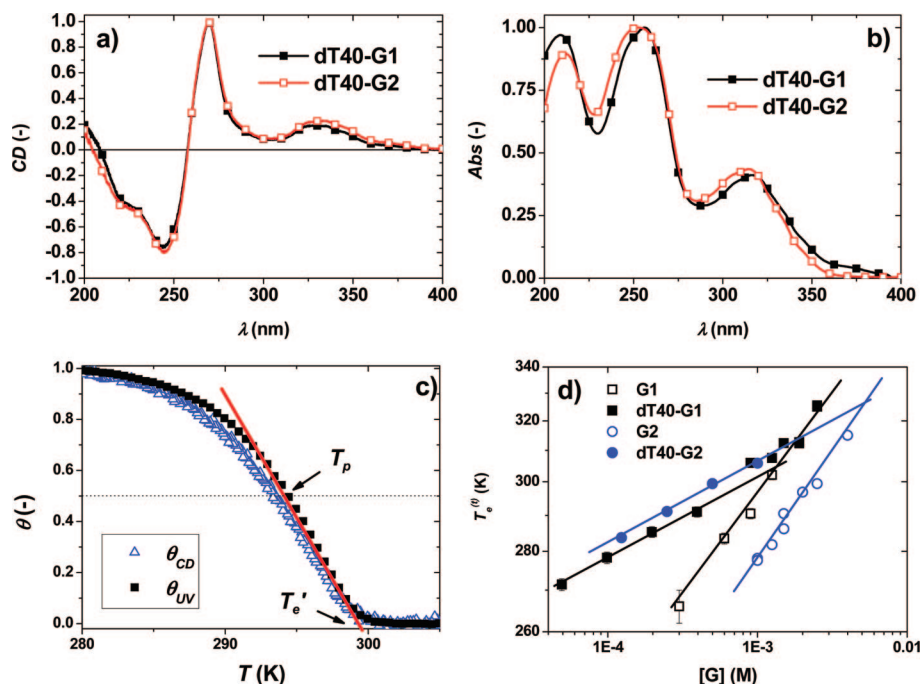

Figure 2. (a) Normalized CD spectra of **G−dT40** mixtures in water. (b) Normalized UV−vis spectra of **G−dT40** mixtures in water. (c) Determination of T_p and T_e^t for [**dT40**] = 6.25 μM and [**G2**] = 0.5 mM. The CD intensity and absorption were measured at $\lambda = 340$ nm. (d) T_e and T_e^t as functions of the guest concentration determined via temperature-dependent UV−vis measurements on **G** and 1:40 **dT40−G** mixtures, respectively, at 269 nm.

Scheme 1. Schematic Representation of the ssDNA-Templated Self-Assembly and the Molecular Structures of the Host Template **dT**q and the Guests **G1** and **G2**
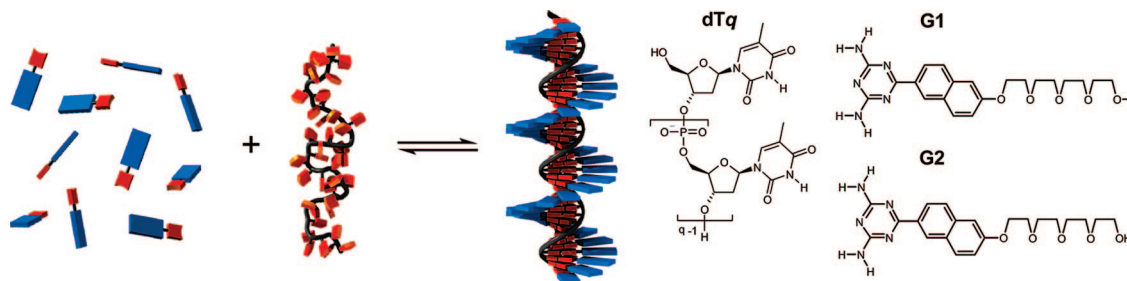
G1[12] by monitoring the hypochromicity upon cooling for different concentrations (Figures 1a and 2d).[5h,i] Similar to **G1** at a concentration of 1 mM,[12] **G2** can aggregate at low temperatures, as evidenced by the hypochromicities at 269 and 320 nm and the scattering above 370 nm (Figure 1a). When the sample is cooled while the UV absorption is continuously monitored, a sharp exponential transition is observed that is indicative of a cooperative self-assembly process.[5h,i] We call

this transition temperature the *elongation temperature*, T_e, at which the self-assembly starts.[5h,i] Compared to **G1**, **G2** exhibits the same kind of cooperative self-assembly, albeit at a T_e value that is 10 °C lower at the same concentration of dissolved material. The enthalpy of elongation, ΔH_e, which is calculated from the slope of a plot of the natural logarithm of the guest concentration [**G**] versus $1/T_e$, is very similar for **G2** (−28 kJ/mol) and **G1** (−27 kJ/mol).[15] Cryo-transmission electron

microscopy (cryo-TEM) images of a **G1** solution with a 1 mM concentration (Figure 1b) revealed micrometer-long laterally interacting fibers of **G1** with a width of 3 nm, which corresponds to the length of one **G1** molecule. A similar solution of **G2** does not show fibers, since **G2** is molecularly dissolved at this temperature and concentration (Figure 1a).

Templated Self-Assembly. When **G2** was mixed with **dT40** in a 40:1 ratio in water at a concentration at which **G2** is molecularly dissolved, a hypochromicity, red-shift, and Cotton effect in the naphthalene absorption region similar to those reported previously for the right-handed **G1**−**dT40** complex were observed (Figure 2a,b).[16] Furthermore, the absorption onset for the **G1**−**dT40** mixture is red-shifted compared with that of the **G2**−**dT40** mixture, which can possibly be attributed to scattering due to large particles in the **G1**−**dT40** solution (see the discussion of the light-scattering experiments, below). To compare the reversible templated self-assembly of **G1** and **G2**, the assembly process was monitored by temperature-dependent UV−vis and circular dichroism (CD) measurements starting from high temperatures at which both components are molecularly dissolved. As the sample is cooled while its absorbance is measured at 340 nm, both the formation of the Cotton effect and the red shift can be monitored as a function of the temperature (Figure 2c).[17] This yields a cooperative buildup[5h,i] of the helically bound fraction θ_{CD} determined by CD, which overlaps with the fraction of bound sites θ_{UV} obtained from the increase in UV absorption, i.e., $\theta_{UV} \approx \theta_{CD}$. This implies that binding almost immediately gives rise to a helical arrangement of the complex formed by single-stranded DNA (ssDNA) and bound guest molecules.

Characteristic of each mixture are its templated polymerization temperature T_p (see below), the temperature at which half of the template binding sites are occupied by guest monomers, and the apparent elongation temperature T_e^t, the temperature at which the straight line through the temperature-dependent data points with the maximum slope crosses the temperature axis (see Figure 2c).[17] T_e^t for the templated assembly is comparable to the elongation temperature T_e for nontemplated cooperative self-assembly discussed above.[12a] The quantity $1/T_e^t$ shows a linear relation with the logarithm of the guest concentration, as does $1/T_e$ (Figure 2d). Comparing **G1** with **G2** shows that the removal of the methyl group not only decreased the naphthalene self-assembly temperature T_e but also slightly increased the **dT40**−**G** self-assembly temperature T_e^t (Figure 2d). The concentration range where the nontemplated self-assembly of **G2** interferes with the templated self-assembly therefore lies at higher concentrations than that for **G1**.
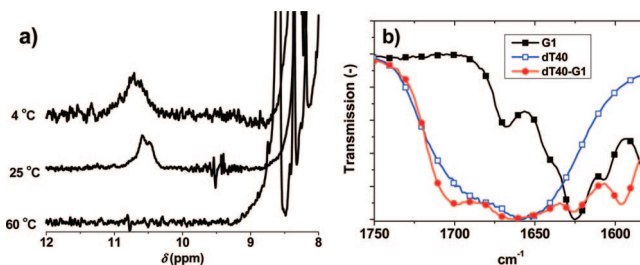
Figure 3. (a) ^{1}H NMR spectra at various temperatures for a **dT40**−**G2** mixture with [**dT40**] = 9 μM and [**G2**] = 1.8 mM. (b) ATR-IR spectra of dried films on glass obtained from solutions of **dT40**, **G1**, and 1:40 **dT40**−**G1**.

Characterization of the dT40−G Complexes. We previously characterized the **dT40**−**G1** complex with UV−vis and CD spectroscopy.[12] Here, the **dT40**−**G1** and **dT40**−**G2** complexes were characterized in more detail using cryo-TEM, ^{1}H NMR and infrared spectroscopy, light scattering, and atomic force microscopy (AFM). To see whether hydrogen bonds in the **dT40**−**G2** complex could directly be detected, ^{1}H NMR spectra using Watergate 3−9−13 solvent suppression were obtained in 9:1 H_2O/D_2O at **G2** and **dT40** concentrations of 1.8 mM and 9 μM, respectively (Figure 3a).[12,18,19] The imino protons of the thymine bases of **dT40** in water can only be detected when they are hydrogen-bonded.[20] At 60 °C, the rapidly exchanging imino protons of the thymines were not detected. When the sample was cooled to 25 °C, the imino-proton signal appeared at 10.5 ppm, indicating hydrogen bonding. This signal shifted further downfield to 10.7 ppm upon cooling to 4 °C. The fact that this signal was sharp indicates that the complexes are still mobile and that they are neither polydisperse nor very large.[31] When the sample was heated back to 60 °C, the imino-proton signal disappeared again, showing the reversibility of the self-assembly process. The NMR data show that **G2** binds to **dT40** at 25 °C, which is in agreement with the optical data (Figure 2d). Hydrogen bonding was further evidenced by attenuated total reflection infrared (ATR-IR) spectroscopy on films obtained by drying a **dT40**−**G** solution in D_2O (Figure 3b), which revealed that the C=O stretch was shifted from 1656 cm^{-1} (for **dT40**) to 1666 and 1702 cm^{-1}, which is typical for hydrogen-bonded thymines.[8b]

To visualize the templated self-assemblies, cryo-TEM was performed.[21] In the case of **G2**−**dT40**, small objects with diameters of 4−5 nm[22] and lengths varying between 5 and 30 nm were observed (Figure 4a). For the **G1**−**dT40** mixture (Figure 4b), similar diameters of 4−5 nm were observed, but here the objects appeared to be more elongated and laterally

(15) In principle, ΔH_e can be determined by fitting the temperature-dependent data with the model for cooperative self-assembly. However, we found that because of a second process, the calculated enthalpy of the temperature-dependent measurements increases with the concentration and deviates from the enthalpy found via the concentration-dependent T_e measurement. Possibly the lateral interactions present between strands of **G** (see the cryo-TEM image) give rise to an additional decrease in absorption intensity and therefore a higher enthalpy.

(16) Previous titration experiments have shown that one **G1** binds to one thymine (see ref 12a). We have found similar results for **G2** (Figure 7a).

(17) In this experiment, a nonstoichiometric ratio was used in order to determine T_p more accurately. It should be noted that T_e^t does not change with the ratio between the guest and the thymine while T_p shows a linear trend with the logarithm of this ratio. T_e^t depends on the guest concentration, while T_p also depends on the template concentration. See the Supporting Information.

(18) The **G1**−**dT40** mixture at this concentration was not suitable for detecting hydrogen bonds because the mixture precipitated during the measurements and thus gave only very broad signals at temperatures where aggregates are formed.

(19) Previously, we have shown with ESI-MS that **G1** binds to oligo-thymines via hydrogen bonding (see ref 12b). We obtained similar results for **G2**; see the Supporting Information.

(20) Cahen, P.; Luhmer, M.; Fontaine, C.; Morat, C.; Reisse, J.; Bartik, K. *Biophys. J.* **2000**, *78*, 1059–1069.

(21) It should be noted that for concentrations and temperatures where the complexes are not formed, no objects could be observed with cryo-TEM. Furthermore, at room temperature and at these concentrations of **G1** and **G2**, the molecules were molecularly dissolved, and therefore, no structures were observed with cryo-TEM.

(22) Similar dimensions have been observed with AFM in the liquid cell. See the Supporting Information and: Surin, M.; Janssen, P. G. A.; Lazzaroni, R.; Meijer, E. W.; Schenning, A. P. H. J. *Adv. Mater.*, in press; DOI: 10.1002/adma.200801701.
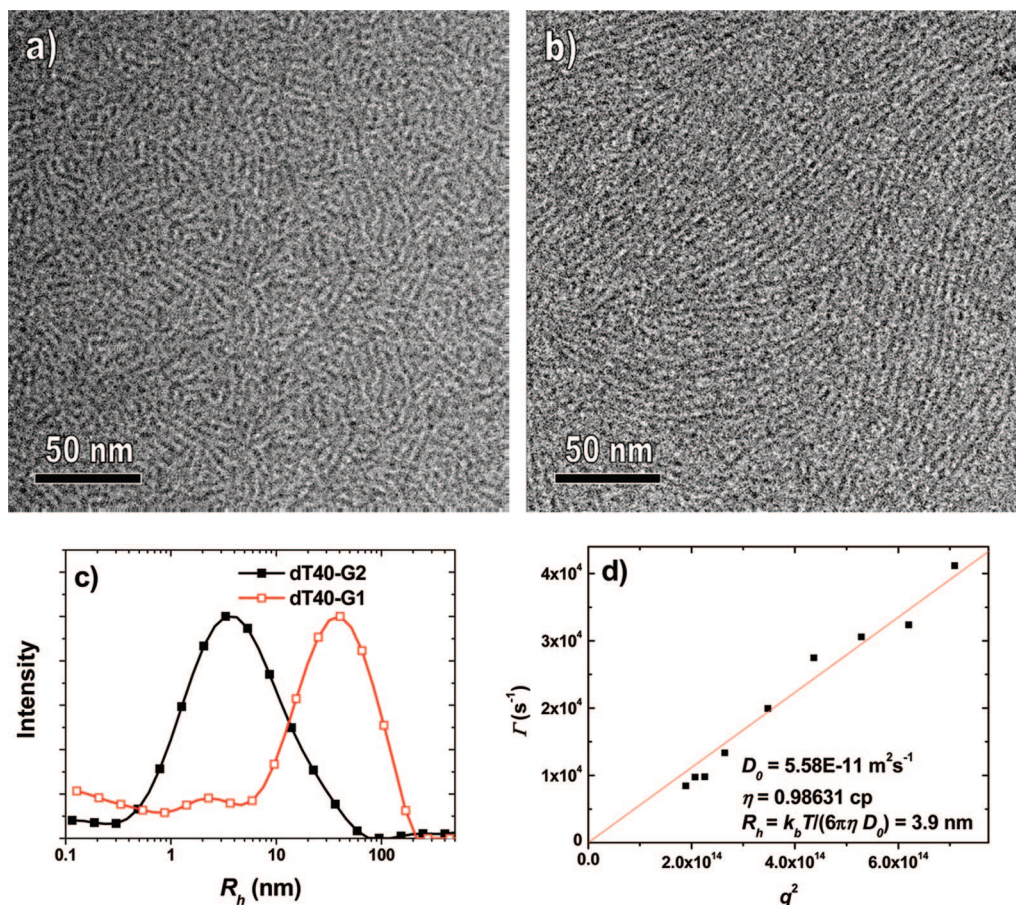
Figure 4. Cryo-TEM micrographs of (a) **dT40−G2** ([**G2**] = 0.8 mM and [**dT40**] = 20 μM) and (b) **dT40−G1** ([**G1**] = 0.8 mM and [**dT40**] = 20 μM) vitrified at 288 K in MilliQ water. (c) Intensity-weighted size distributions for **dT40−G2** and **dT40−G1** mixtures ([**G**] = 0.8 mM and [**dT40**] = 10 μM) at 294 K obtained using DLS at 90°. (d) Decay rate (Γ) as a function of q^2 determined via angle-dependent DLS and the corresponding linear fit for the mixture with [**G2**] = 0.8 mM and [**dT40**] = 10 μM at 294 K.

aggregated, supporting the hydrodynamic radius (R_h) value of 40 nm estimated from the DLS measurements (see below). The measured diameter of 4−5 nm agrees well with the calculated diameter obtained from the molecular dynamics simulations, which revealed helical complexes with a diameter of 4.5 nm and a length of 14 nm (see below). The measured lengths of the **G2−dT40** complexes varied around the expected **dT40** length of 14 nm, which could be due to a random orientation as a result of the vitrification process and overlap of aggregates due to the sample thickness of at least 100 nm.[23] Extended aggregation or incomplete filling of templates could also cause such an effect (see below). AFM images of **G1−dT40** mixtures in a liquid cell show objects with heights of ∼2.7 nm and widths with tip convolution[24] of 20−35 nm, similar to what was found for **dTp−G2** mixtures in a liquid cell.[26]

The complexes were further characterized by light-scattering measurements. DLS at 90° revealed an intensity-weighted average R_h value of 40 nm for the **G1−dT40** complex, while the **G2−dT40** complex has an R_h value of 4 nm (Figure 4c). The latter value agrees with the 3.9 ± 0.1 nm value of R_h found with angle-dependent DLS (Figure 4d). The size of the **G1−dT40** complex is much larger than the expected 5 nm,

suggesting that the assembled structures further aggregate into larger assemblies, as previously seen with cryo-TEM (Figure 4b). The existence of larger particles also explains the apparent red-shift in the absorption onset for **G1−dT40** due to scattering from the **G1−dT40** complexes, which are larger than the **G2−dT40** complexes. The R_h values of the **dT40−G2** aggregates are close to the R_h value of 5 nm calculated for a single **dT40−G2** complex assuming a cylindrical structure.[25] The small difference might be due to the fact that the complex is not a perfectly filled cylinder, which would result in an experimentally determined radius that is smaller than the calculated R_h for a perfectly filled cylinder. The static light scattering (SLS) experiments on the **dT40−G2** aggregates showed that the intensity was independent of the angle, indicating that the sample consists predominantly of small particles.[26] The scattering intensity at smaller scattering vectors was not accurate enough to determine the radius of gyration, and therefore, the aspect ratio of the assemblies could not be determined. A temperature-dependent SLS intensity measure-

(23) Vos, M. R. J.; Bomans, P. H. H.; de Haas, F.; Frederik, P. M.; Jansen, J. A.; Nolte, R. J. M.; Sommerdijk, N. A. J. M. *J. Am. Chem. Soc.* **2007**, *129*, 11894−11895.
(24) Bustamante, C.; Vesenka, J.; Tang, C. L.; Rees, W.; Guthold, M.; Keller, R. *Biochemistry* **1992**, *31*, 22−26.

(25) For the calculation of R_h, we used $D_0 = k_B T/6\pi\eta R_h = k_B T(\ln\rho + 0.3 + 0.4738/\rho + 0.4167/\rho^2 - 0.3394/\rho^3)/6\pi\eta b'$, in which D_0 is the diffusion coefficient, η is the coefficient of viscosity, $b' = L/2$, and $\rho = L/(2r)$, where $L = 14$ nm is the length from the MD simulations and $r = (4.5$ nm$)/2 = 2.25$ nm is the radius from the MD simulations. See: (a) Tirado, M. M.; Garcia de la Torre, J. *J. Chem. Phys.* **1979**, *71*, 2581−2587. (b) Santos, N. C.; Castanho, M. A. R. B. *Biophys. J.* **1996**, *71*, 1641−1650.
(26) See the Supporting Information.

ment revealed a reversible transition at 310 K, above which the intensity dropped to the intensity of a **dT40** solution.[27] The transition temperature observed with SLS corresponds well with what was also observed in the temperature-dependent UV and CD data.[26] The light-scattering experiments show that there is little or no higher-order aggregation occurring for these **dT40**−**G2** aggregates, as observed with the cryo-TEM experiments. Thus, removing the methyl group not only suppresses the nontemplated self-assembly of the guests without decreasing the binding affinity to **dT40** but also prevents further aggregation of the **dT40**−**G** complexes.

Molecular Modeling. In order to gain more insight into the supramolecular organization in the DNA hybrid assemblies, molecular mechanics (MM) calculations and molecular dynamics (MD) simulations were performed.[28] An MM calculation shows that the lowest-energy conformation of a diaminotriazine moiety binding to the thymine base consists of the expected three H bonds, while the adenine−thymine (**A**−**T**) base pair and the diaminotriazine−diaminotriazine pair both have two H bonds.[29]

To characterize the structure of the **G1**−**dT40** complex, MD simulations with the CHARMm force field[26,30] were performed using the generalized Born implicit water solvent model. We started the MD simulations with the complex obtained from MM calculations on a **G1**−**dT40** complex built up from a right-handed B-helix DNA structure. Two types of structure were considered with the implicit water solvent model: (1) one without counterions bound to the phosphate groups along the oligonucleotide backbone, in which the global structure carries a total charge of −40e due to the phosphate backbone; and (2) one with 40 Na$^+$ counterions, each bound to a phosphate group along the DNA backbone, in which the global system is therefore neutral.[28] These latter two extremes were considered for comparison and because the **dT40** aqueous solutions were measured both in buffered solution and in ultrapure water. It should be noted that even in ultrapure water, counterions are bound to the phosphate.

In the MD simulation, the structure without the counterions tends to stretch because of Coulomb repulsion between the phosphate groups, but this is balanced by π stacking of the naphthalenes, maintaining a 14.5 nm long right-handed helix with three turns, a pitch of 13−14 **G1** units, and a rotation per "base pair" of ~27° (Figure 5a). In this conformation, adjacent naphthalenes overlap and are parallel to each other (Figure 5a) but perpendicular to the strand axis. The ethylene oxide side chains remain extended, interacting with each other only slightly.

The MD simulations performed on **dT40**−**G1** with Na$^+$ counterions show that the **dT40** right-handed helix is stabilized in a B-helix-like right-handed conformation with four turns, a pitch of 10 **G1** units, and a rotation per "base pair" of 36°; the
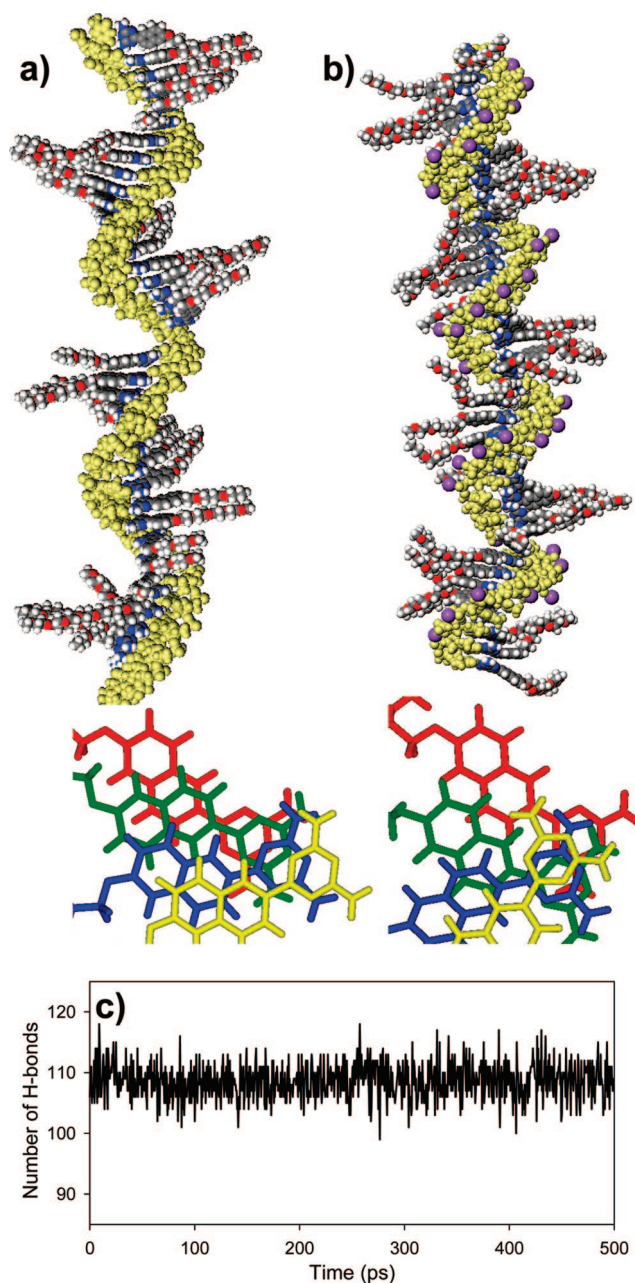
(27) It should be noted that the scattering intensity of a **dT40** solution is almost the same as that of ultrapure water. Therefore, it does not allow for a reliable calculation of R_h.

(28) A related study on two different guests binding to **dT40** or **dT20** model stacks with Na$^+$ counterions has been published. See ref 22.

(29) Although the absolute values have no meaning, the comparison of the hydrogen bonding energies, as estimated in vacuum with the Dreiding force field (see: Mayo, S. L.; Olafson, B. D.; Goddard, W. A. *J. Phys. Chem.* **1990**, *94*, 8897–909.), give a clue about the relative amplitudes of the interactions: for **G**−**T**, **A**−**T** and **G**−**G** pairs, this value amounts to −45, −29, and −26 kJ/mol, respectively.

(30) *CHARMm Force Field*, version 22; Accelrys: San Diego, CA, 2006; Momany, F. A.; Rone, R. *J. Comput. Chem.* **1992**, *13*, 888–900.

(31) Saenger, W. *Principles of Nucleic Acid Structure*; Springer-Verlag: New York, 1984; p 556.

Figure 5. CPK models of snapshots from an MD simulation optimized with MM of the **G1**−**dT40** complex (a) without and (b) with Na$^+$ counterions (mauve) along the ssDNA backbone. The bottom figures show stacks of four **G1** units inside the assemblies in (a) and (b), illustrating the packing of the naphthalene units in the corresponding models above. (c) Evolution of the number of H bonds during the last 500 ps of the MD run for the model with counterions.

length of the stack varies around 13.3 nm (Figure 5b). Remarkably, adjacent naphthalenes do not or only slightly overlap (Figure 5b) and are not all parallel. The thymines are much closer than in the previous case without Na$^+$ counterions, giving rise to multiple H bonds between each diaminotriazine and adjacent thymines as a result of base flipping. The number of intermolecular H bonds in the system (Figure 5c) fluctuates between 100 and 120 during the MD run (simulation at 263 K) with an average of ~110 H bonds, illustrating that this structure is clearly stabilized by H bonds between neighboring **G1** molecules and thymines rather than by the poor π stacking between the naphthalenes.[26] By subtraction of the enthalpy of
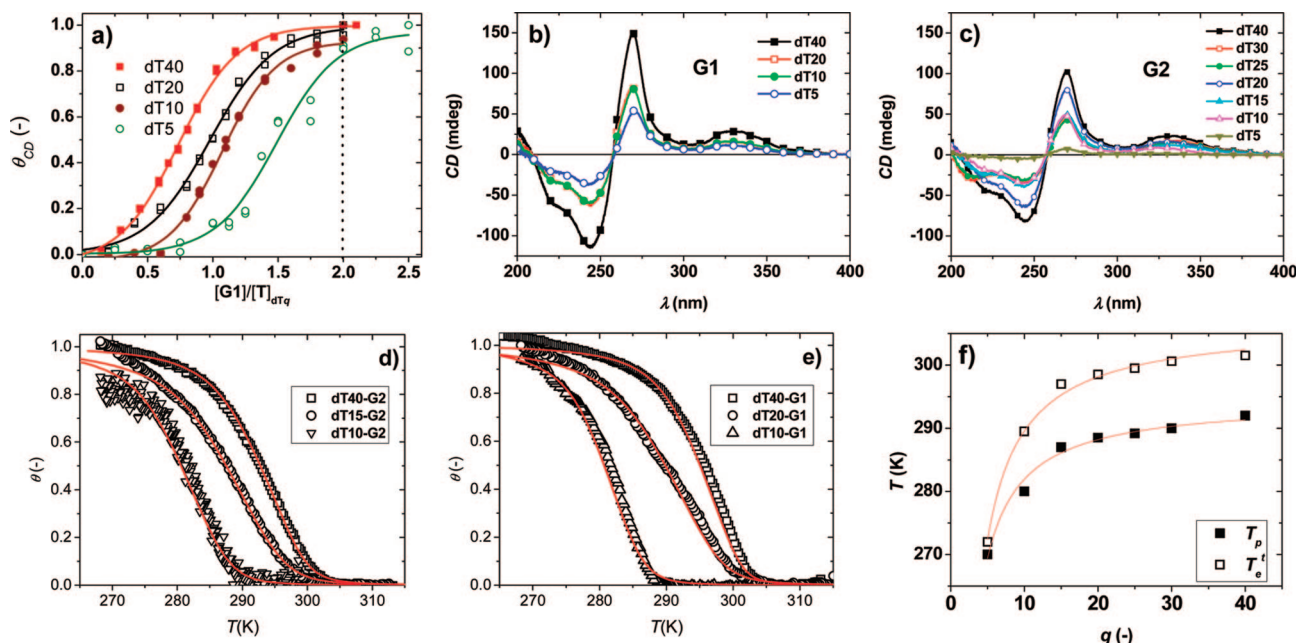
Figure 6. (a) Titration of **G1** into **dTq** (q = 5, 10, 20, 40) measured via the CD intensity at 327 nm at 263 K. The lines have been added to guide the eye. The dotted line indicates 2 equiv of **G1** with respect to thymine. (b, c) CD spectra of (b) **G1**−**dTq** and (c) **G2**−**dTq** mixtures at 268 K. For **G1**, the host binding site concentration was [**H**] = 0.25 mM and [**G1**] = 0.5 mM. For **G2**, [**H**] = 0.2 mM and [**G2**] = 0.4 mM. (d, e) Fraction of occupied sites θ as a function of temperature for different **dTq** template lengths q for (d) **G2** and (e) **G1**. The stoichiometric guest−host binding site ratio was [**G**]/[**H**] = 2, with [**H**] = 0.2 mM for **G2** and [**H**] = 0.25 mM for **G1**. The absorption was measured at 269 nm for **G1** and 340 nm for **G2**. The red lines show the fits to the model. (f) T_{p} and $T_{\mathrm{e}}^{\mathrm{t}}$ as functions of q for **G2**. The stoichiometric ratio was [**G**]/[**H**] = 2 and [**H**] = 0.2 mM. The red lines are fits to the functions $T_{\mathrm{p}}(q) = T_{\mathrm{p}}(\infty) + A_{\mathrm{p}}/q$ and $T_{\mathrm{e}}^{\mathrm{t}}(q) = T_{\mathrm{e}}^{\mathrm{t}}(\infty) + A_{\mathrm{e}}/q$, where A_{p} and A_{e} are constants.
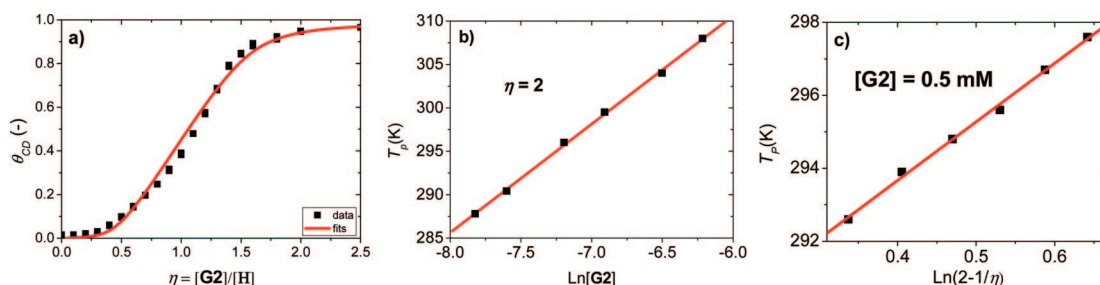
Figure 7. (a) Titration of **G2** into **dT40**: θ_{CD} as a function of $\eta = $ [**G2**]/[**H**] for **dT40**−**G2** mixtures with [**H**] = 0.08 mM at λ = 269 nm and T = 268 K. (b) The polymerization temperature T_{p} of **G2**−**dT40** mixtures as a function of ln [**G2**] with η fixed at 2 results in a straight line. (c) The polymerization temperature T_{p} of **G2**−**dT40** mixtures as a function of ln(2 − 1/η) with [**G**] fixed at 0.5 mM results in a straight line. The red lines are fits to the model.

each single molecule from the total enthalpy of the assembly, the enthalpy change per monomer due to binding, Δh, in the presence of Na$^+$ was estimated with CHARMm to be −54 kJ/mol. In both cases considered here, the simulations are consistent with the existence of right-handed helices, in agreement with the CD measurements. The radius of gyration, as estimated from the molecular models, is significantly different for the two types of structure considered: 4.47 nm without Na$^+$ (Figure 5a) and 4.09 nm with Na$^+$ (Figure 5b). The latter is in agreement with the hydrodynamic radius estimated from the DLS experiments (R_{h} = 3.9 ± 0.1 nm).

Different Template Lengths. Having analyzed the self-assembly of **dT40** and **G** in detail, we next investigated the influence of the length of the template on the self-assembly process, with the final goal of obtaining control over the size of the assemblies. Titration studies of **G1** and **G2** with **dTq** (q = 5, 10, 20, 40) measured with UV−vis[26] and CD spectroscopy at 263 K (Figures 6a and 7a) show that saturation of the signal occurs at [**G**]/[**H**] ratios greater than 1, where [**H**] is the host binding site concentration. For smaller template sizes, the

binding of guest molecules is less efficient, and more than stoichiometric amounts of guest molecules are needed to get a high degree of binding. This suggests that guest−guest interactions occurring on the template are important for stabilizing the complexes (see below). At least 2 equiv of guests must be present in order to compare the Cotton effects of the **G**−**dTq** complexes (Figure 6a). All of the **G**−**dTq** mixtures have similarly shaped Cotton effects at 263 K, but the intensity decreases upon going to smaller templates (Figure 6b,c), suggesting that the CD intensity depends on the template length. The stabilizing effect of larger templates is further evidenced by temperature-dependent UV measurements (Figure 6d,e). For larger templates, a larger total amount of guest−guest interaction is present for each template, thereby increasing the stability of the stack. The steep decline in $T_{\mathrm{e}}^{\mathrm{t}}$ for small q shows that a certain size of the template is needed to stabilize the hybrid complex (Figure 6f). This is also known to be true for the helix−coil transition in biopolymers and in fact also for the formation of a double strand in DNA, for which at least four bases are needed to have favorable hybridization.[26,31] End effects quite generally

Scheme 2. Schematic Drawing of the Ising Chain Model for Templated Supramolecular Polymerization[a]
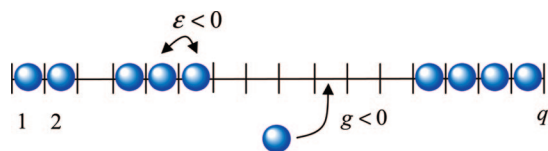
[a] The guest molecules (blue balls) adsorb onto a template having q binding sites, with a negative binding free energy, g. If two guests bind at neighboring sites on the template, they interact according to a stacking free energy, ε, which is also negative for the cooperative case. Each bound molecule also represents chemical work that enters the model through the chemical potential of the guest molecules in the solution.

destabilize ordered configurations in polymeric objects because groups near the ends have fewer interactions with neighbors. This makes chain ends more statistically disordered than the central parts.

Model for Templated Self-Assembly. To determine how the guests are distributed on the different template lengths, we developed a mathematical model that can be used to fit the experimental data for guests binding to a finite-sized template. We use a two-parameter model that is based on the one-dimensional (1D) Ising model for ferromagnetism and is similar in spirit to the binding model put forward by McGhee and von Hippel[32] as well as to the Zimm−Bragg model for the helical transition in biopolymers.[14] It provides a coarse-grained description of the process of binding guest molecules to a template of finite size in terms of g, the free energy for binding between a guest and a binding site on a host template, and ε, the free energy for stacking of two bound monomers (Scheme 2). It should be noted that we use one energy for the guest−guest interaction and another for the host−guest interaction in our 1D Ising model. This assumption seems appropriate to describe the experimental data (see below). If a guest molecule is bound to a template site, its free energy is lowered by the binding free energy g, and if two neighboring sites are occupied, the free energy of the system is additionally altered by the stacking free energy ε, which is negative for cooperative guest binding and positive for anticooperative guest binding. The interplay between the free energies ε and g determines the distribution of bound guests across the template molecule, i.e., the way the templates are filled as function of the fraction of occupied binding sites, θ. When all of the template binding sites are occupied, $\theta \equiv 1$. When the stacking free energy ε is much smaller than the thermal energy $k_B T$, the guest molecules are equally dispersed over the entire template. A relatively high stacking free energy ε makes the assembly process more cooperative in the sense that binding of monomers next to each other is favored. The fractions of empty and filled templates are then set by mass action, i.e., the concentration and the guest−template stoichiometry. A brief description of the model and its validation with the experimental data is given below. Fitting the data with this model also provides an estimate of the enthalpy and entropy of binding that make up the binding free energy. The model does not account for additional processes such as two or more guest−guest or host−guest interaction energies, self-aggregation, or higher-order aggregation. The template **dTq** is modeled as a quasi-1D string with q binding sites. Each binding site represents a thymine of **dTq** and can be either empty or occupied by one guest molecule.

The fraction of occupied sites, θ, is a function of g, ε, q, temperature, and the template and guest concentrations. θ is experimentally determined via the normalized change in UV absorption, a measure of guest binding that is assumed to be proportional to θ. It should be noted that the normalized change in UV−vis absorption is proportional to the fraction of bound sites on the template, θ_{UV}, while the change in CD intensity is proportional to the helical fraction of the occupied sites, θ_{CD}, which in principle can be smaller than θ_{UV}. In our case, we do not see a significant difference between θ_{CD} and θ_{UV} (Figure 2c). The experiments show that templated supramolecular polymerization occurs only below a certain transition temperature, T_e^t. For definiteness, the transition temperature from nonoccupied templates to fully occupied templates, T_p, is defined as the temperature at which half of the template binding sites are occupied by guest monomers [i.e., $\theta(T_p) \equiv {}^1/_2$] and can be determined directly from the temperature-dependent measurements of θ (Figure 2c).

We tested and validated whether our model is applicable for ssDNA-templated self-assembly by analyzing independent types of experiments: length-, temperature-, concentration-, and host−guest-ratio-dependent measurements (Figures 6 and 7). A detailed description of the model and the fitting procedures can be found in the Supporting Information. We first tested the influence of the length of the template with temperature-dependent measurements. The fraction of occupied sites, θ, as a function of temperature shows an increase in T_p with the template length q for both **G1** and **G2** (Figure 6d,e). Decreasing the template size allows the size of the aggregates to be controlled, but lower temperatures are needed to get a high coverage (large θ). Analysis of our model shows that 100% binding can be achieved only when $\eta \geq 1$, where $\eta = [\mathbf{G}]/[\mathbf{H}]$ is the stoichiometric ratio and $[\mathbf{H}]$ is the thymine host binding site concentration; in other words, an excess of guest monomers over host binding sites is required. Therefore, we used an excess of guests ($\eta = 2$) to make sure that we obtained full coverage at low enough temperatures. Fitting the data yielded $\Delta h(T_p) \approx -19 k_B T_p$ and $\varepsilon \approx -5.5 k_B T_p$ for **G2** and $\Delta h(T_p) \approx -22 k_B T_p$ and $\varepsilon \approx -5.1 k_B T_p$ for **G1**, independent of the template length q, within experimental error, corresponding to values of -47, -14, -55, and -13 kJ/mol, respectively, at $T_p = 300$ K. The very close values of binding enthalpy and stacking free energy for the two types of guests shows the similarity in the cooperative nature of the interactions of the guests with the template, and thus, a similar structure can be expected for all q. The experimental enthalpy of binding for **G1**, $\Delta h(T_p) \approx -22 k_B T_p = -55$ kJ/mol, is remarkably close to the value found with the MD simulations for the system with counterions, $\Delta h(263 \text{ K}) \approx -54$ kJ/mol.

The model furthermore predicts that the polymerization temperature T_p is inversely proportional to q, the length of the template. The obtained value of T_p as defined above as a function of q is in good agreement with the model, as evidenced by the good fit to the functional form of $T_p(q) = T_p(\infty) + A_p/q$, even down to $q = 5$ (Figure 6f), where A_p is a constant. Also, T_e^t has the same functional dependence on q as T_p, albeit with a different constant A_e, as expected theoretically. In principle, q of a host of unknown length can be determined via the transition temperatures of a calibrated set of lengths and host and guest concentrations. In the case of a calibration with T_e^t, this can be done irrespective of the host concentration, since the value of T_e^t depends only on the guest concentration and the length q.[26]

(32) McGhee, J. D.; von Hippel, P. H. *J. Mol. Biol.* **1974**, *86*, 469–489.

Table 1. Summary of the Average Fitting Parameters (in units of k_BT_p), As Determined by Comparison with Our Experimental Data, Showing the Similarity of the Parameters for **G1** and **G2**

guest monomer	ε	g	$\Delta h(T_p)$	$T_p\Delta S(T_p)$
G1	-5.1 ± 0.3	-10 ± 1	-22 ± 2	-12 ± 2
G2	-5.3 ± 0.3	-9 ± 1	-20 ± 2	-11 ± 2

For the titration of **G2** into a **dT40** template solution at a fixed temperature, the change in CD intensity was used to determine θ (Figure 7a). Again, the model fit very well with the data, and the binding and stacking free energy values were extracted ($g \approx -9k_BT_p$ and $\varepsilon \approx -5.1k_BT_p$, respectively), revealing a cooperative templated self-assembly process. The stacking free energy value obtained here is comparable to the value extracted from temperature-dependent UV absorption curve. Combining the binding free energy, $g \approx -9k_BT_p$, with the enthalpy change for binding to the template, $\Delta h(T_p) \approx -19k_BT_p$, gives an estimate of $T_p\Delta S(T_p) \approx -10k_BT_p$ for the entropy loss due to the organization of monomers on the template as a result of binding. This entropy loss upon binding is therefore quite appreciable. We speculate that this must also be attributed in part to the loss of conformational freedom of the backbone ssDNA chain.

In the model, we can also describe the dependence of T_p on the host and guest concentrations for large enough templates. This allows for a direct determination of the enthalpy change per monomer upon binding to the template, Δh, from the measured T_p at different concentrations with a fixed η ratio (Figure 7b) or at different ratios at a fixed guest concentration (Figure 7c).[26,33,34] The slope (α) of the plot of T_p versus the natural logarithm of the guest concentration, ln [**G2**], was used to estimate the enthalpy change via the relation $\alpha = -kT_p^2/\Delta h(T_p)$, yielding $\Delta h(T_p) \approx -21.5k_BT_p$. Similarly, the slope ($\alpha$) of the plot of T_p versus $\ln(2 - 1/\eta)$ yielded $\Delta h(T_p) \approx -18k_BT_p$. Both values are in agreement with the enthalpy value obtained from fitting θ as function of temperature, $\Delta h(T_p) \approx -19k_BT_p$.

We can conclude that our coarse-grained 1D Ising model is able to describe the nature of the self-assembly process and shows good self-consistency and good agreement with the experimental data (Table 1). Therefore, we now use the experimentally obtained guest−guest interaction ε to get a qualitative, theoretical picture of how the guests are distributed over the templates by considering the correlation length, which is defined as the number of correlated template binding sites: in our case, the correlation length is a measure of the number of template sites filled one after the other. The correlation length $\xi = \xi(q, T, ...)$ depends not only on the fraction of bound sites but also on the interaction between the guests on the template. For our purposes, it is useful to focus on ξ_0, the value of the correlation length of bound guest molecules in the idealized case of an infinitely long template ($q \rightarrow \infty$), for conditions exactly at the polymerization transition temperature, so $T = T_p$. We might call this the "bare", underlying correlation length, which acts as a reference value and explains the existence of two regimes for how the guests distribute over the template. Our model predicts that for the template lengths shorter than this correlation length, i.e., for $q < \xi_0$, the assembly process is in essence all-or-nothing at T_p. This means that at T_p these

templates in the solution are either filled or empty: mixed forms are not favored because of a lack of combinatorial entropy on account of the fact that there are in that case fewer mutually distinguishable distributions of bound guest molecules on the template. On the other hand, for template lengths that are longer than the bare correlation length, i.e., for $q > \xi_0$, the templates have alternating filled and bound sections with lengths on the order ξ_0 at T_p: the combinatorial factor can benefit from a large number of entropically favorable fragmentations on a long chain. Of course, the fraction and the *actual* correlation length decrease below the transition temperature and increase above it.

The bare correlation length as defined above can be shown to obey the relation $\xi_0 \approx \frac{1}{2}\sigma^{-1/2}$, where $\sigma = e^\varepsilon$ is a measure of the cooperativity of the templated polymerization transition and ε is in units of thermal energy k_BT_p.[14,35] For example, if the polymerization transition becomes sharper, this is caused by a stronger cooperative guest−guest interaction; ε becomes more negative, and hence, σ becomes smaller, i.e., more cooperative, implying that ξ_0 becomes larger. Because we obtained ε at T_p (Table 1), we can calculate the correlation length exactly at the polymerization transition temperature T_p: the ε value gives $\sigma \approx 4 \times 10^{-3}$, which in turn yields the correlation length $\xi_0 \approx 8$ for **G2**. This means that according to our model, the average length of bound sections at T_p is ~ 8.[36] For **G2** binding to **dTq**, we therefore expect the small templates **dT5** and **dT10** to be either filled or empty at temperatures close to T_p. For the long templates **dT20**, **dT30**, and **dT40** close to T_p, we expect to get alternating sequences of filled and empty sections upon binding, with domains having a length on the order of the correlation length ξ_0.[37] For a complete qualitative theoretical picture of the dominant configurations of the template for **G2**, we constructed a phase diagram based on the fitting results of the model, in which we indicated the fraction of occupied template binding sites θ (contour lines) as a function of the length of the template (vertical axis) and a measure of the concentration or temperature (horizontal axis); this diagram is shown in Figure 8.[38]

Conclusion

We have characterized the structure and templated self-assembly process of two naphthalene derivatives binding to ssDNA templates of different lengths using a combined experimental and theoretical approach. The supramolecular stack of guest molecules binds to the ssDNA via hydrogen bonding and is held together by $\pi−\pi$ and hydrophobic interactions. The removal of the terminal methyl group of the ethylene oxide tail of the guest suppresses nontemplated aggregation but also

(33) It should be noted that changing the ratio at a fixed guest concentration hardly affects T_e^t. See the Supporting Information.

(34) In principle, T_p can be estimated directly from the data without the necessity of fitting the data to the coarse-grained model.

(35) Goldenfeld, N. *Lectures on Phase Transitions and the Renormalization Group*; Addison-Wesley: Boston, 1992; p 394.

(36) The correlation length ξ_0 here is defined exactly at the polymerization transition for the idealized case of an infinitely long chain. For template sizes $q > \xi_0$, $\xi_0 \approx \xi$ is reasonably accurate. For template sizes $q < \xi_0$, ξ decreases with q.

(37) For these long template lengths, a predominance of completely filled templates is present only at high template coverages of, say, $\theta > 0.9$, where the *actual* correlation length ξ approaches infinity.

(38) The theoretical model provides us with much more information about the details of the system than only gross averages, which can be of great value for the practical applications of templated self-assemblies. In principle, our coarse-grained model can be used to calculate the way that the guest monomers are distributed over the templates quantitatively as a function of q and θ via an implicit set of equations (see the Supporting Information). For ease of calculation and clarity, we chose to directly construct a qualitative picture of the dominant configurations of the occupation of the templates by relating the binding energies ε and g with q and θ, similar to what was done by Zimm and Bragg[14] for the helix−coil transition in polypeptides.
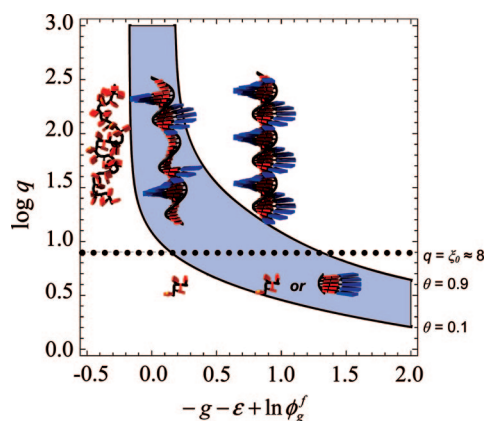
Figure 8. Configuration-state diagram of the template for **G2** as a function of the template length q and the mass-action variable $-g - \varepsilon + \ln \phi_g^f$, which is actually a chemical potential and a measure of the concentration of the guest molecules or the temperature of the solution. In the mass-action variable, the stacking free energy ε and the binding free energy g are in units of thermal energy $k_B T_p$, and ϕ_g^f is the concentration of free guest molecules. Shown are results calculated for **G2** and stoichiometric ratios $\eta \geq 2$, obtained from fitting the data with the model. The two contours of constant θ are the (arbitrarily chosen) boundaries of the transition region from sparely bound to densely bound guest molecules. The black dotted line shows $q = \xi_0$. It should be noted that the width of the transition region varies as the template length q changes. For very long templates ($q \gg \xi_0$), the width is proportional to $\sigma^{1/2}$ at T_p. For short templates ($q < \xi_0$), the width is proportional to $\sigma^{-1/q}$ at T_p.

prevents further aggregation of the templated complexes. The experimental findings on the binding of the guest to the ssDNA template show good agreement with our self-consistent model for templated self-assembly as well as with molecular dynamics simulations. For long enough templates, the most important parameters (host−guest and guest−guest interaction energies) for templated self-assembly can be obtained from just two sets of experiments: a guest titration and a concentration- or stoichiometric-ratio-dependent measurement of the transition temperature. Together with the enthalpy of binding, a prediction can be made for the transition temperature for any given concentration of guest and template. The obtained guest−guest and host−guest interaction parameters provide qualitative information on the size distribution and the efficiency of covering whole templates, yielding a correlation length of 8 at the polymerization temperature. This indicates that template sizes below this length will be filled one-by-one at the transition temperature. Ideally, the correlation length could be further improved by increasing the attractive interactions between the guest molecules. Our study, in which an ssDNA was used as a template for the self-assembly of a water-soluble functional molecule equipped with an appropriate hydrogen-bonding moiety and a model description was included, provides insights into how tape-measure molecules can be used to create nanoscale objects of uniform length. These insights are of great importance for templated supramolecular polymerizations in both synthetic chemistry and biology.

Supporting Information Available: Complete ref 5b; full experimental section, including general methods, materials, the synthetic route and details of **G2**, and general sample preparation methods; temperature-dependent CD, DLS, and UV measurements, the SLS experiment, ESI-MS spectra, AFM micrographs, and cryo-TEM micrographs; and details concerning the MD simulations and the model for templated polymerization. This material is available free of charge via the Internet at http://pubs.acs.org.

JA808075H